



*Supplement of*

**East Asian methane emissions inferred from high-resolution inversions of GOSAT and TROPOMI observations: a comparative and evaluative analysis**

**Ruosi Liang et al.**

*Correspondence to:* Yuzhong Zhang (zhangyuzhong@westlake.edu.cn)

The copyright of individual parts of the supplement might differ from the article licence.

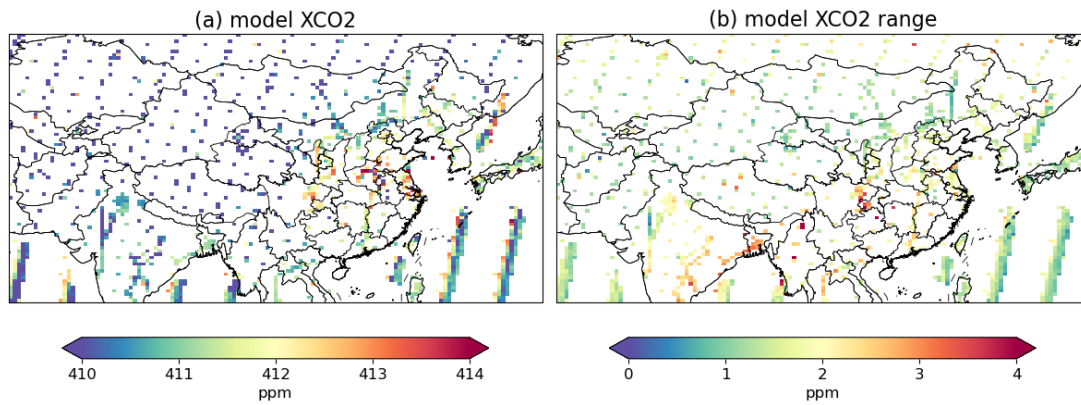


**Figure S1: XCO<sub>2</sub> model data used in proxy method. (a) Model XCO<sub>2</sub> component of the final proxy data product; (b) Maximum difference (in ppm) between model XCO<sub>2</sub> from GEOS-Chem, CarbonTracker and LMDZ.**

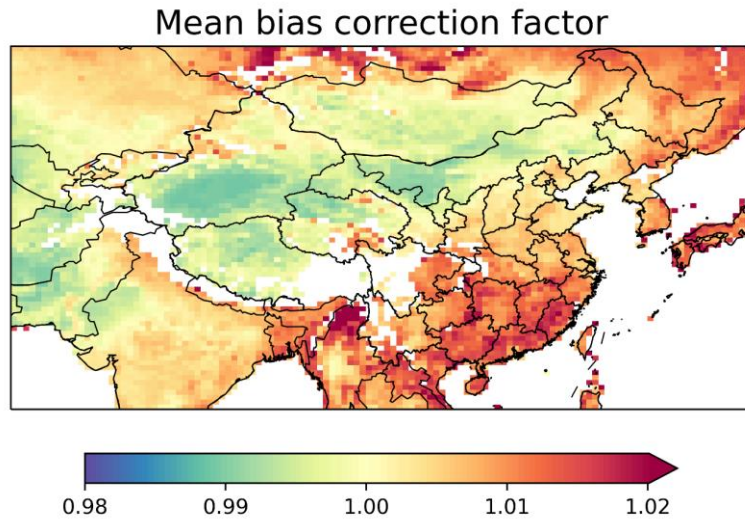


**Figure S2: Bias correction factor derived by Lorente et al. (2021) for original TROPOMI XCH<sub>4</sub> retrievals.**

The spatial distribution of gridded daily observation numbers

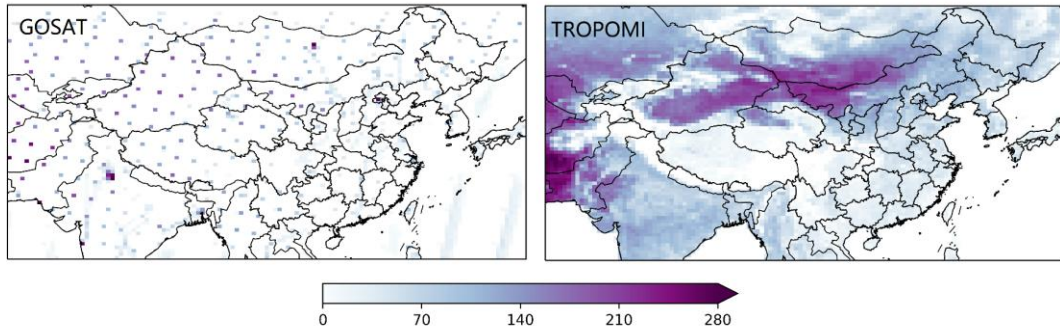


**Figure S3: Numbers of gridded daily average observations for GOSAT and TROPOMI during 2019.**

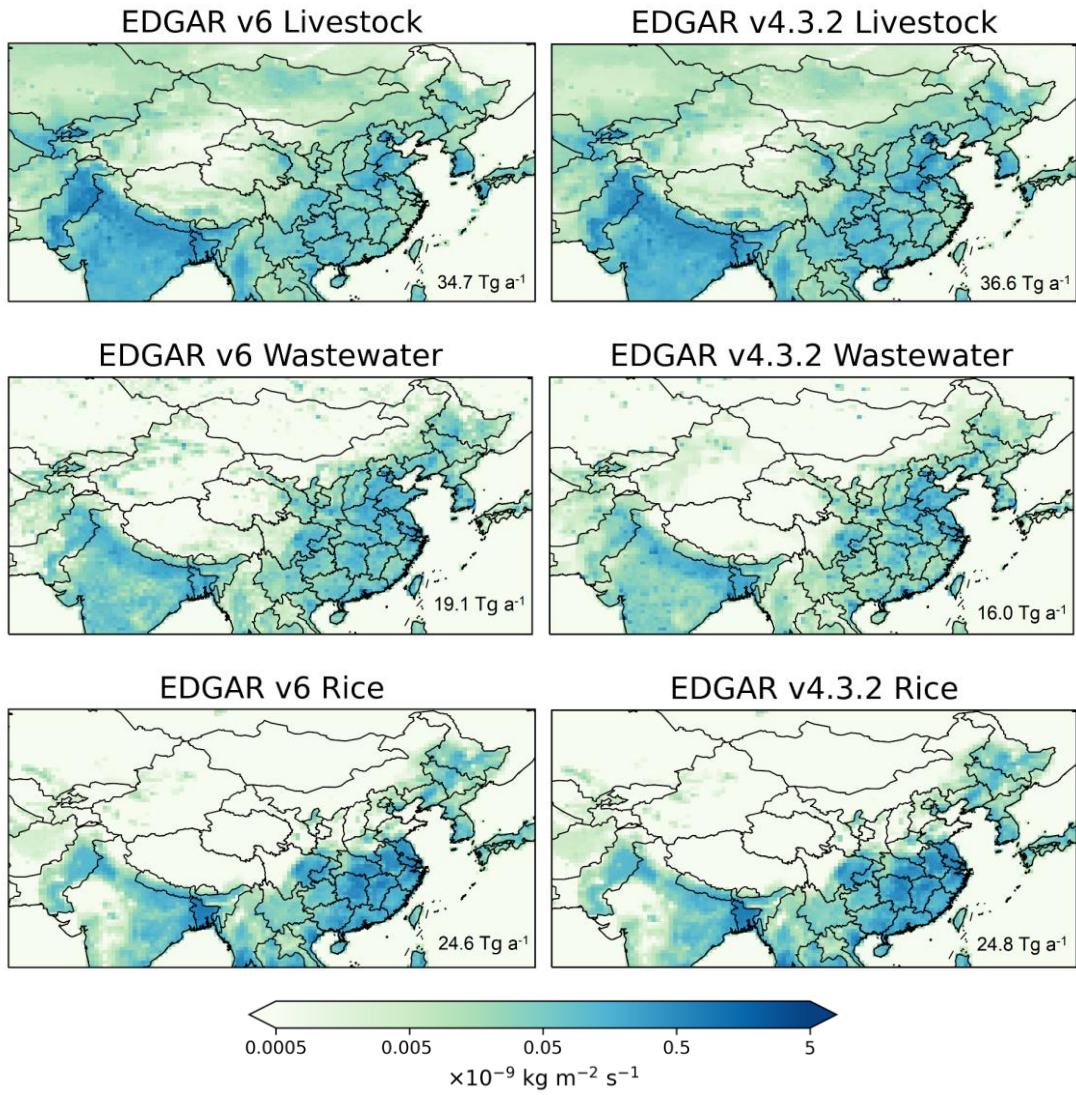


**Figure S4: Comparison of the three main sectors (Livestock, Wastewater, Rice) provided by EDGAR v6.0 and EDGAR v4.3.2.**

600 clusters

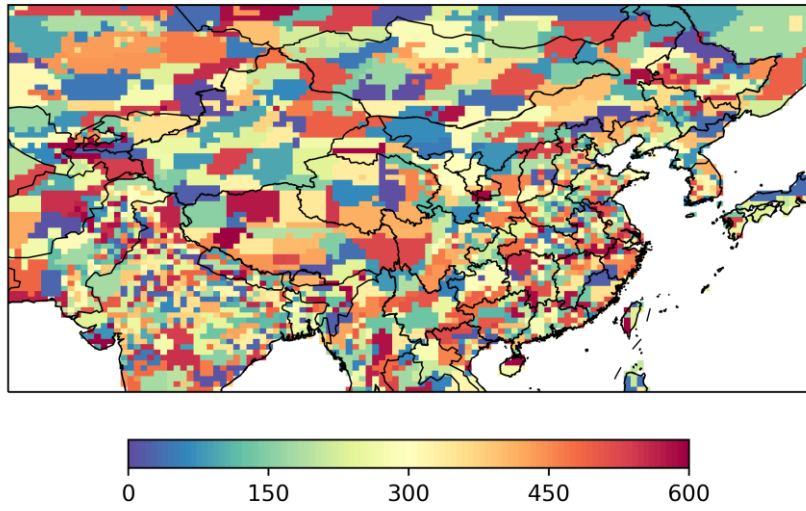


**Figure S5: Map of 600 clusters for the state vector of the inversion.**

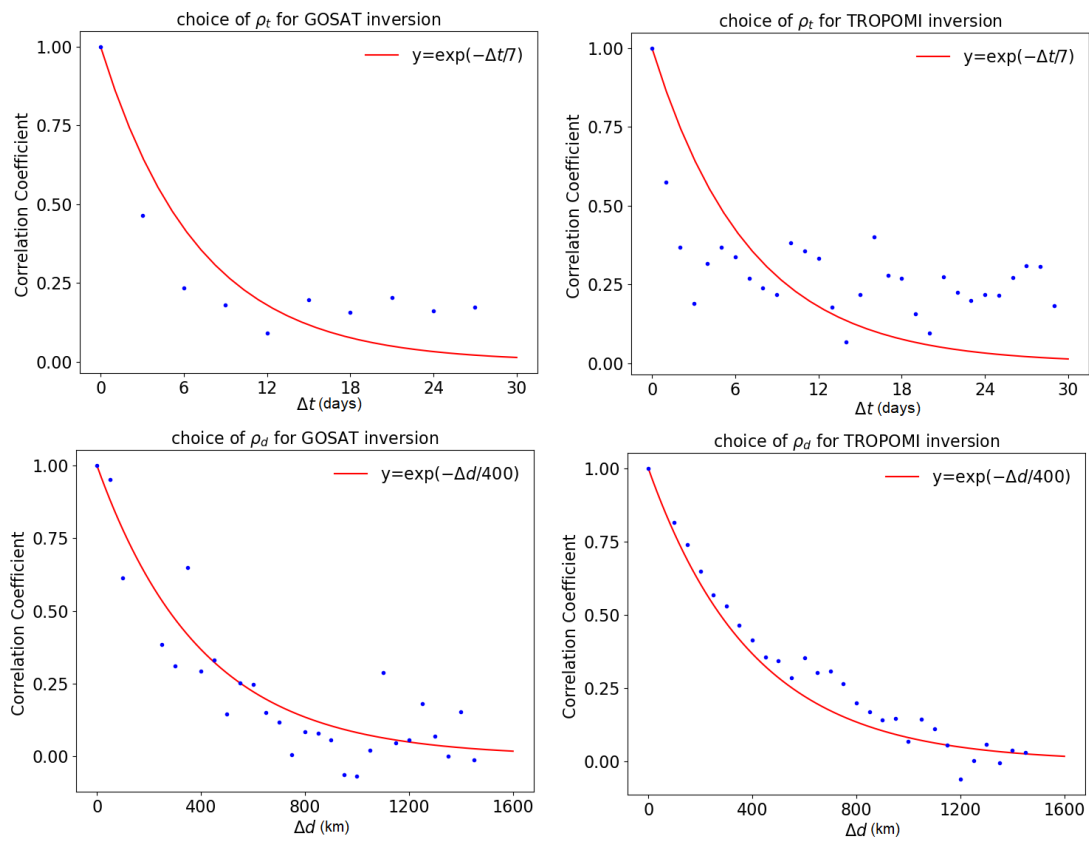


**Figure S6: Determination of two parameters  $\rho_t$  and  $\rho_d$  values. Correlation coefficients of prior residual errors are computed as a function of distance and time interval (blue dots). Left panel is for GOSAT data and right for TROPOMI data.**

### The choice of the regularization parameter $\gamma$

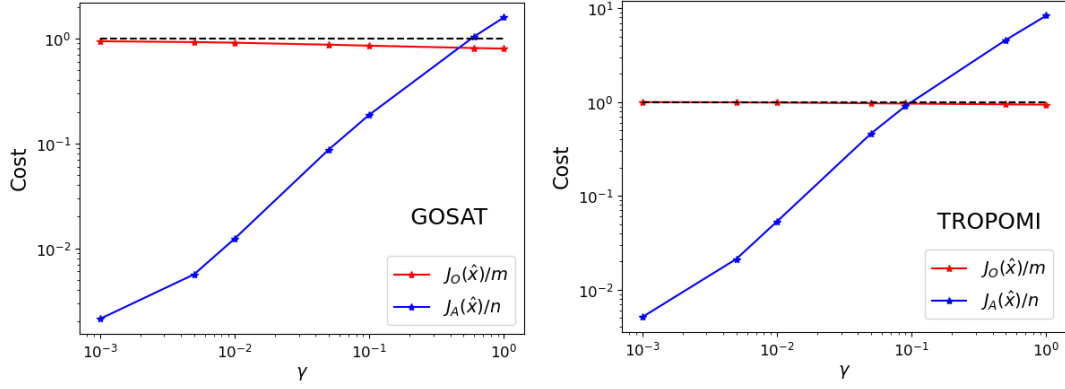


**Figure S7: Determination of the regularization parameter.** The prior term  $J_A(\hat{x}) = (\hat{x} - x_A)^T S_A^{-1} (\hat{x} - x_A)$  and the observation term  $J_O(\hat{x}) = (y - K\hat{x})^T S_0^{-1} (y - K\hat{x})$  as a function of  $\gamma$ .  $n$  is the dimension of the state vector and  $m$  is the dimension of the observation vector. Left panel is for the GOSAT inversion and right panel for the TROPOMI inversion. We chose  $\gamma = 0.09$  for TROPOMI inversion and  $\gamma = 0.6$  for GOSAT inversion.



Results of a set of sensitivity inversions (posterior - prior emissions)

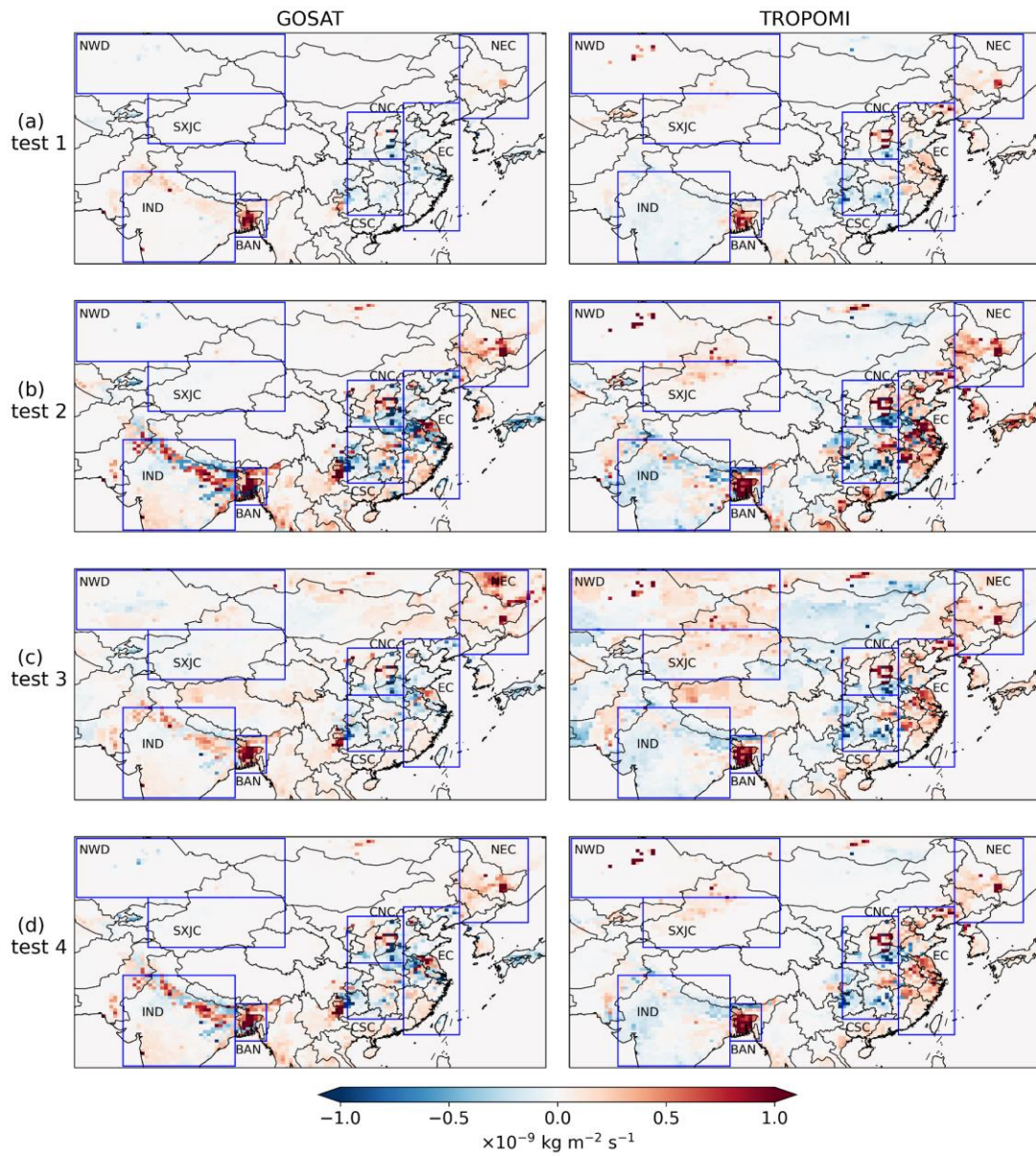


**Figure S8: Correction of annual-average methane emissions relative to the prior emissions (posterior - prior), inferred by a set of sensitivity inversions (Left panel: GOSAT, Right panel: TROPOMI). (a) test 1: emissions are optimized seasonally instead of annually; (b) test 2: increasing prior error standard deviations from 50% to 100%; (c) test 3: a minimum absolute prior error standard deviation is set to be  $1 \times 10^{-10} \text{ kg m}^{-2} \text{ s}^{-1}$ ; (d) test 4: applying regularization factor ( $\gamma = 0.6$  for GOSAT and  $\gamma = 0.09$  for TROPOMI) to account for error correlations in  $S_0$  instead of the method proposed in Section 3.3.**

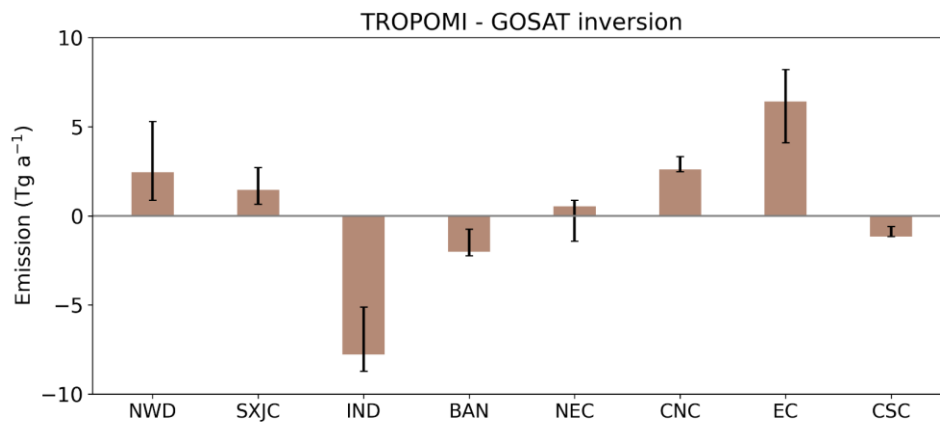


**Figure S9: The difference in regional methane emissions inferred by GOSAT and TROPOMI inversions. Bars represent the results from the main inversion, and error bars represent the range of the sensitivity inversions.**

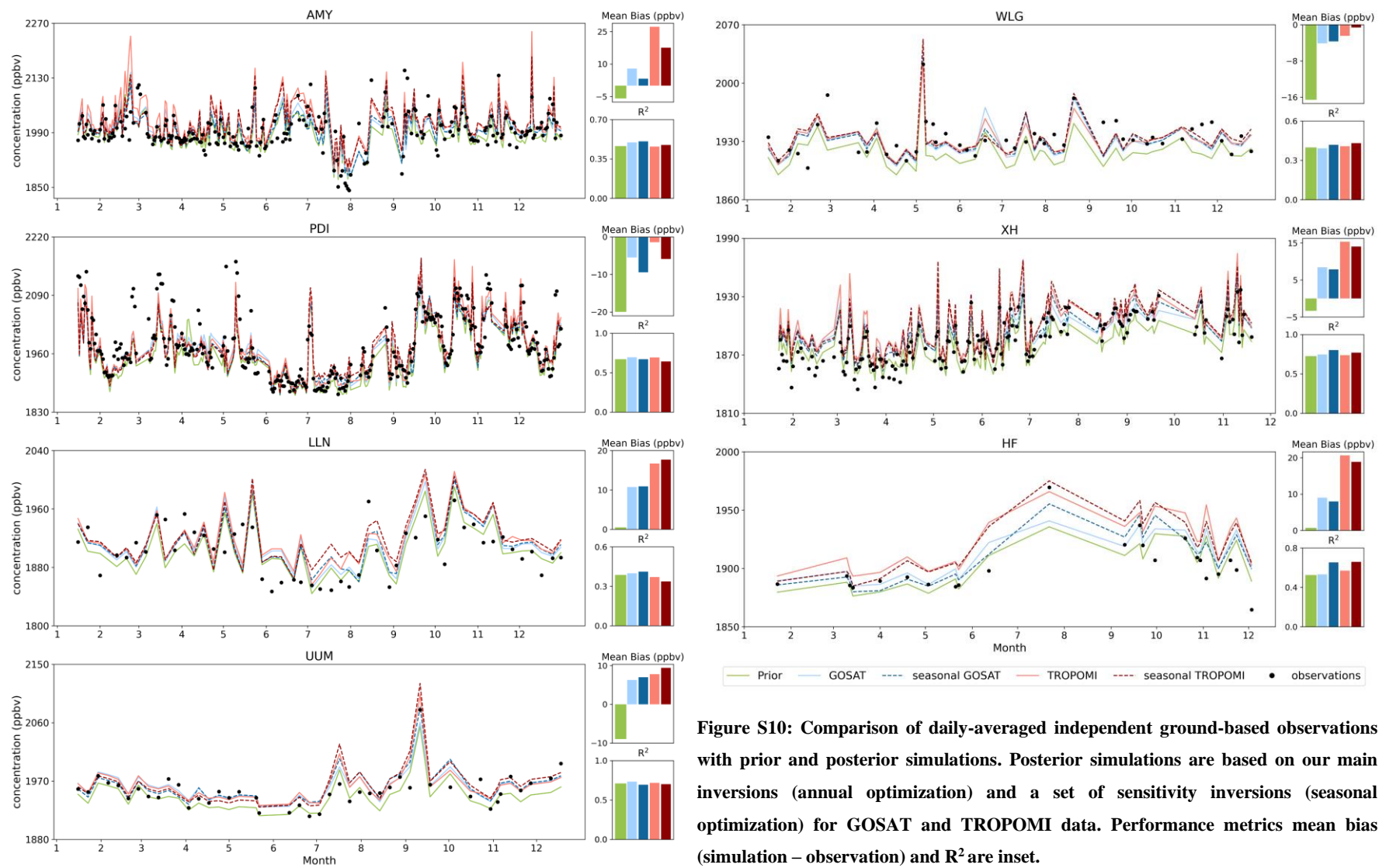


**Figure S10: Comparison of daily-averaged independent ground-based observations with prior and posterior simulations. Posterior simulations are based on our main inversions (annual optimization) and a set of sensitivity inversions (seasonal optimization) for GOSAT and TROPOMI data. Performance metrics mean bias (simulation – observation) and  $R^2$  are inset.**

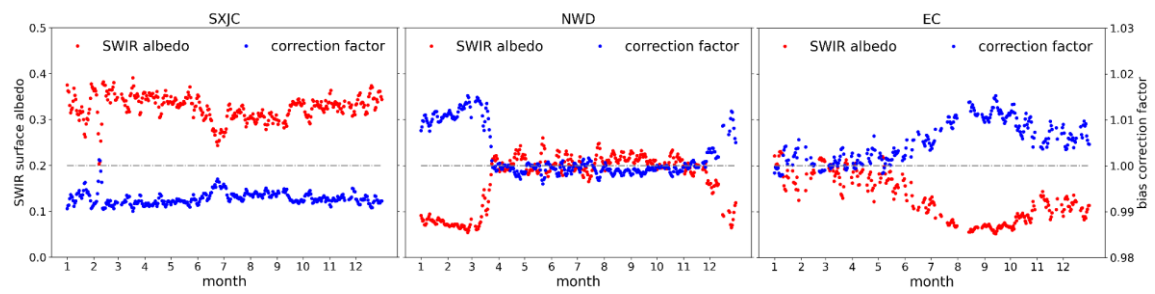


**Figure S11: Time series of average surface albedo and bias correction factor over SXJC, NWD and EC. The bias correction algorithm used in this TROPOMI product is a function of the SWIR effective surface albedo where the correction factor is forced to be 1 at surface albedo around 0.2. When the surface albedo is less than 0.2, the bias correction factor is greater than 1, and otherwise the bias correction factor is less than 1.**

Comparison of coincident GOSAT and original TROPOMI data

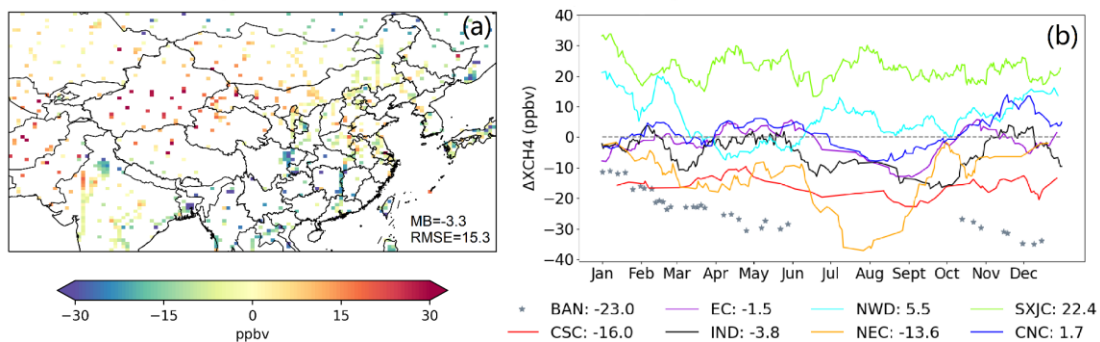


**Figure S12: Average differences in XCH<sub>4</sub> between GOSAT and original (not bias-corrected) TROPOMI (TROPOMI – GOSAT) shown on the 0.5° × 0.625° grid (a) and by region (b). Annual averages of regional differences (in ppbv) are inset in Panel (b).**

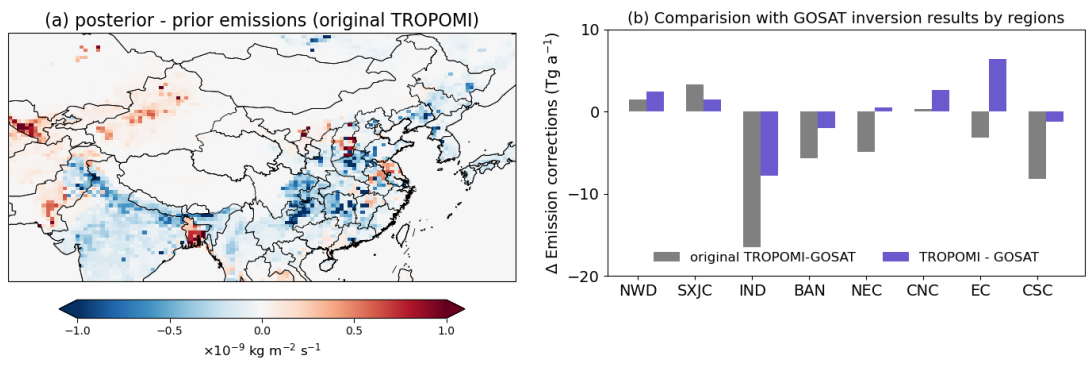


**Figure S13: Results of inversions of original TROPOMI retrievals without application of the bias correction scheme. Panel (a) shows the adjustment to prior emissions by this inversion. Panel (b) compares regional inversion results using original and bias-corrected TROPOMI data, relative to the GOSAT inversion results.**

**Table S1: Surface observation sites used for evaluation**

Site	Code	Lon	Lat	Alt(m)	Measurements
Anmyeon-do, South Korea	AMY	126.33	36.54	87	Hourly & daily, <i>in situ</i>
Pha Din, Vietnam	PDI	103.52	21.57	1478	Hourly & daily, <i>in situ</i>
Lulin, Taiwan China	LLN	120.87	23.47	2867	Weekly, flask
Ulaan Uul, Mongolia	UUM	110.10	44.45	1012	Weekly, flask
Waliguan, China	WLG	100.89	36.29	3815	Weekly, flask
Xianghe, China	XH	116.96	39.75	36	Hourly & daily, FTIR total column measurements
Hefei, China	HF	117.17	31.9	30	Hourly & daily, FTIR total column measurements

**Table S2: Mean 2019 methane emissions used in GEOS-Chem<sup>a</sup>**

Sources Type (Tg a <sup>-1</sup> )	China <sup>b</sup>		East Asia <sup>c</sup>			
	Prior	Posterior		Prior	Posterior	
		TROPOMI	GOSAT		TROPOMI	GOSAT
<b>Anthropogenic</b>						
Oil	1.0	1.6	1.1	1.5	2.1	1.7
Gas	0.2	0.2	0.2	3.6	3.7	3.8
Coal	16.6	17.8	15.6	19.4	21.8	18.3
Livestock	11.9	12.8	12.4	36.6	36.7	40.9
Landfill	2.9	3.1	2.8	5.1	5.6	5.6
Wastewater	8.1	8.8	8.1	16.0	16.9	17.7
Rice	14.5	16.9	15.3	24.8	29.5	28.9
Others	6.1	6.7	6.1	9.6	10.2	10.2
<b>Natural</b>						
Biomass burning	0.3	0.3	0.3	1.8	2.1	2.1
Wetlands	3.2	4.1	3.4	9.1	11.3	10.7
Seeps	0.3	0.5	0.3	0.7	0.9	0.7
Termites	0.8	0.9	0.8	1.8	1.9	2.0
<b>Total source<sup>d</sup></b>						
Anthropogenic	61.3	67.9 ± 0.9	61.6 ± 1.0	116.7	126.5 ± 1.1	127.1 ± 1.4
Natural	4.5	5.8 ± 0.2	4.8 ± 0.3	13.4	16.2 ± 0.4	15.5 ± 0.4
All	65.8	73.7 ± 0.9	66.4 ± 1.1	130.0	142.7 ± 1.3	142.6 ± 1.5

<sup>a</sup> Mean 2019 values of methane sources in China and the whole inversion domain. It contains prior emissions described above and posterior emissions obtained by two inversions using TROPOMI and GOSAT observations respectively.

<sup>b</sup> Methane emissions in China.

<sup>c</sup> Methane emissions in the entire East Asian domain.

<sup>d</sup> Uncertainties are showed here ( $1\sigma$  standard deviations derived from posterior error covariance matrices).



## Reference

Lorente, A., Borsdorff, T., Butz, A., Hasekamp, O. P., aan de Brugh, J., Schneider, A., Wu, L., Hase, F., Kivi, R., Wunch, D., Pollard, D. F., Shiomi, K., Deutscher, N. M., Velasco, V. A., Roehl, C. M., Wennberg, P. O., Warneke, T., and Landgraf, J.: Methane retrieved from TROPOMI: improvement of the data product and validation of the first 2 years of measurements, *Atmos. Meas. Tech.*, 14, 665-684, <https://doi.org/10.5194/amt-14-665-2021>, 2021.